Cyclic RGD Peptides Containing β-Turn Mimetics

Roland Haubner,[†] Wolfgang Schmitt,[†] Günter Hölzemann,[‡] Simon L. Goodman,[‡] Alfred Jonczyk,[‡] and Horst Kessler*[,†]

Contribution from the Institute of Organic Chemistry and Biochemistry, TU München, Lichtenbergstrasse 4, D-85747 Garching, Germany, and Merck KGaA Preclinical Research, Frankfurter Strasse 250, D-64271 Darmstadt, Germany

Received March 18, 1996[⊗]

Abstract: The $\alpha_V\beta_3$-receptor, one member of the integrin family, is implicated in angiogenesis and in human tumor metastasis. Spatial screening led to the highly active first-generation peptide c(RGDfV), which shows a βII′/γ-turn arrangement with D-Phe in the $i + 1$ position of the βII′-turn. Further reduction of the flexibility should be achieved by incorporating different rigid building blocks (turn mimetics) like the (*S*)- and (*R*)-Gly[ANC-2]Leu dipeptide, the β-turn dipeptide (BTD) and the (*S,S*)-spiro-Pro-Leu moiety. These distinct β-turn mimetics are introduced by replacing the D-Phe-Val dipeptide in the lead structure c(RGDfV). In peptide analogues c(RGD"*S*-ANC") (**PA1**), c(RGD"*R*-ANC") (**PA2**), and c(RGD"BTD") (**PA3**) the turn mimetic does not adopt the desired position in the β-turn, instead Gly occupies the $i + 1$ position of the βII′-turn. Only c(RGD"spiro") **PA4** led to the desired βII′/γ-turn arrangement with the turn motif in the $i + 1$ and $i + 2$ position of the β-turn. These effects may arise from particular steric effects of the cyclic pentapeptide system in combination with steric requirements of the ANC and BTD moiety. Additional investigations on cyclic hexapeptide derivatives show that the BTD occupies the expected $i + 1$ and $i + 2$ position of a βII′-turn in these systems. Structure−activity investigations showed that the incorporation of the rigid turn motifs could not reduce the flexibility of the RGD site (ANC and BTD) or fix a conformation which is unable to match the receptor very well (spiro). On the other hand, recent findings that the proton of the amide bond between Asp and the following amino acid is essential for high activity can be confirmed. Moreover, the synthesis of c(RGD"*R*-ANC") **PA2** led to one of the compounds most active in inhibiting vitronectin binding to the $\alpha_V\beta_3$-integrin.

Introduction

Cell−cell and cell−matrix adhesion are important in pathological processes like thrombosis,[1] osteoporosis,[2] and tumor metastasis.[3] One of the major cell surface receptor classes involved in these interactions are the integrins.[4] Each integrin is an integral plasma membrane, heterodimeric glycoprotein consisting of an α-subunit and a smaller β-subunit.[5] The specificity for ligand binding is determined by a particular combination of different α- and β-subunits.

Besides the platelet glycoprotein IIb/IIIa ($\alpha_{IIb}\beta_3$), which is involved in platelet aggregation,[6] the inhibitors of which are used as antithrombotic agents,[7] a vitronectin receptor ($\alpha_V\beta_3$) is of great interest concerning metastasis of tumor cells.[8] There is a striking difference in the expression of the β_3-subunit between tumorigenic and nontumorigenic lesions, when expression of integrins on cells in tissue sections are examined.[9] In addition to the vitronectin receptor, there is a variety of other integrins reported to be expressed on the surface of tumor cells.[10] Furthermore, it was shown that the $\alpha_V\beta_3$-receptor plays a crucial role in the angiogenesis which is important for the development of metastatic colonies.[11] Metastasis of several tumor cell lines[12] as well as tumor-induced angiogenesis[13] can be inhibited by antibodies or small, synthetic peptides acting as ligands for these receptors.

[†] Institut of Organic Chemistry and Biochemistry.
[‡] Merck KGaA Preclinical Research.
[⊗] Abstract published in *Advance ACS Abstracts,* August 1, 1996.

(1) (a) Albelda, S. M.; Buck, C. A. *FASEB J.* **1990**, *4*, 2868−2880. (b) Cox, D.; Aoki, T.; Seki, J.; Motoyama, Y.; Yoshida, K. *Med. Res. Rev.* **1994**, *14*, 195−228.

(2) (a) Denhardt, D. T.; Guo X. *FASEB J.* **1993**, *7*, 1475−1482. (b) Grano, M.; Zigrino, P.; Colucci, S.; Zambonin, G.; Trusolino, L.; Serra, M.; Baldini, N.; Teti, A.; Marchisio, P. C.; Zambonin Zallone, A. *Exp. Cell Res.* **1994**, *212*, 209−218. (c) Chorev, M.; Dresner-Pollak, R.; Eshel, Y.; Rosenblatt, M. *Biopolym. (Pep. Sci.)* **1995**, *37*, 367−375.

(3) (a) Nicolson, G. L. *Biochim. Biophys. Acta* **1982**, *695*, 113−176. (b) Terranova, V. P.; Hujanen, E. S.; Martin, G. R. *J. Natl. Cancer Inst.* **1986**, *77*, 311−316. (c) Liotta, L. A.; Rao, C. N.; Wewer, U.M. *Annu. Rev. Biochem.* **1986**, *55*, 1037−1057. (d) Liotta, L. A. *Cancer Res.* **1986**, *46*, 1−7. (e) Albelda, S. M. *Lab. Invest.* **1993**, *68*, 4−17. (f) Glukhova, M.; Deugnier, M.-A.; Thiery, J. P. *Mol. Med. Today* **1995**, *1*, 84−89.

(4) (a) Hynes, R. O.; Lander, A. D. *Cell* **1992**, *68*, 303−322. (b) Pignatelli, M.; Stamp, G. *Cancer Surv.* **1995**, *24*, 113−127. (c) Cerri, A.; Berti, E. *Eur. J. Dermatol.* **1995**, *5*, 177−185.

(5) (a) Hynes, R. O. *Cell* **1987**, *48*, 549−554. (b) Ruoslathi, E.; Pierschbacher, M. D. *Cell* **1986**, *44*, 517−518. (c) Ruoslathi, E.; Pierschbacher, M. D. *Science* **1987**, *238*, 491−497. (d) D'Souza, S. E.; Ginsberg, M. H.; Plow, E. F. *TIBS* **1991**, *16*, 246−250.

(6) (a) See ref 1. (b) Smith, J. W.; Ruggeri, Z. M.; Kunicki, T. J.; Cheresh, D. A. *J. Biol. Chem.* **1990**, *265*, 12267−12271.

(7) Ojima, I.; Chakravarty, S.; Dong, Q. *Bioorg. Med. Chem.* **1995**, *3*, 337−360, and references therein.

(8) (a) Marshall, J. F.; Nesbitt, S. A.; Helfrich, M. H.; Horton, M. A.; Polakova, K.; Hart, I. R. *Int. J. Cancer* **1991**, *49*, 924−931. (b) Felding-Habermann, B.; Mueller, B. M.; Romerdahl, C. A.; Cheresh D. A. *J. Clin. Invest.* **1992**, *89*, 2018−2022. (c) Nip, J.; Shibata, H.; Loskutoff, D. J.; Cheresh, D. A.; Brodt, P. *J. Clin. Invest.* **1992**, *90*, 1406−1413. (d) Falcioni, R.; Cimino, L.; Gentileschi, M. P.; D'Agnano, I.; Zupi, G.; Kennel, S. J.; Sacchi, A. *Exptl. Cell Res.* **1994**, *210*, 113−122. (e) Lafrenie, R. M.; Gallo, S.; Podor, T. J.; Buchanan, M. R.; Orr, F. W. *Eur. J. Cancer* **1994**, *30A*, 2151−2158. (f) Kawahara, E. Ooi, A.; Nakanishi, I. *Pathol. Int.* **1995**, *45*, 493−500.

(9) Albelda, S. M.; Motto, S. A.; Elder D. E.; Stewart R.; Damjanovich L.; Herlyn, M.; Buck, C. A. *Cancer Res.* **1990**, *60*, 6757−6764.

(10) (a) Terranova, V. P.; Roa, C. N.; Kalebic, T.; Morgulies, M.; Liotta, L. A. *Proc. Natl. Acad. Sci. USA* **1983**, *80*, 444−448. (b) Wayner, E. A., Carter, W. G. *J. Cell Biol.* **1987**, *105*, 1873−1884. (c) Cheresh, D. A.; Smith, J. W.; Cooper, H. M.; Quaranta, V. *Cell* **1989**, *57*, 59−69.

(11) Brooks, P. C.; Clark, R. A. F.; Cheresh, D. A. *Science* **1994**, *264*, 569−571.

(12) (a) Reference 10b. (b) Ceresh, D. A.; Spiro, R. G. *J. Biol. Chem.* **1987**, *36*, 17703−17711. (c) Humphries, M. J.; Yamada, K. M.; Olden, K. *J. Clin. Invest.* **1988**, *81*, 782−790. (d) Gehlsen, K. R.; Argraves, W. S.; Pierschbacher, M. D.; Ruoslathi, E. *J. Cell Biol.* **1988**, *106*, 925−930.

S0002-7863(96)00875-X CCC: $12.00

All inhibitory peptides contain the amino acid triplet Arg-Gly-Asp (RGD), the so-called "universal cell recognition sequence". This sequence is found in many extracellular matrix proteins like vitronectin, laminin, fibrinogen, and fibronectin.[14] Despite this common sequence, a high substrate specificity among the different integrins is observed. This can be explained by particular conformations of the RGD sequence in different matrix proteins.[5c]

In order to define an antagonist pharmacophore, it is necessary to determine the spatial structure of the active site with high precision. The only known X-ray structure results from the N-terminal A domain of an α-subunit.[15] But neither the structure of a complete integrin nor of a receptor-bound ligand complex is known. The conformations of some proteins containing a biologically relevant RGD sequence (γ-crystalline,[16] tenascin,[17] foot-and-mouth disease virus,[18] and the 10th type III module of fibronectin[19]) as well as of some disintegrins like kistrin,[20] echistatin,[21] and flavoridine[22] have been examined. In addition, the secondary structure elements of albolabrin, another disintegrin, are known.[23] In each structure the RGD sequence is exposed at the tip of a flexible loop or in an extended edge−strand of a β-sheet (γ-crystalline). Recently, the structure of the RGD-containing decorsin,[24] a leech protein, was determined. In contrast to the above mentioned proteins the structure of decorsin is well-defined in the region of the RGD sequence and shows an extended conformation on the tip of a loop, with the side chains of Arg and Asp orientated in almost opposite directions. Decorsin binds to both GPIIb/IIIa and the vitronectin receptor with high affinity. This leads to the assumption that the well-defined RGD loop is still capable of fitting the different receptors. This flexibility of particular RGD motifs prohibits a determination of the bioactive conformation necessary for a structure-based rational drug design.

Because of these problems we indirectly determine the conformation of the active site using small peptides containing the RGD sequence.[25,31] Small linear peptides possess a very high flexibility and are normally not suited for structural analysis.[26] For that reason our group[27] and others[28] use cyclization as a method to reduce the accessible conformational space. Nevertheless, such cyclic peptides can still perform conformational transitions.[29] The introduction of rigid building blocks should further decrease this flexibility.

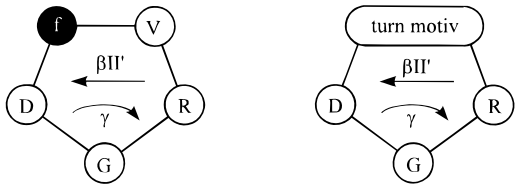

Figure 1. Replacement of the D-Phe-Val dipeptide by several turn motifs to fix the βII′/γ-turn arrangement. The full circle represents a D-amino acid.

Here we describe the incorporation of several known rigid building blocks into cyclic penta- and hexapeptides containing the RGD sequence. Structural influences and consequences concerning the inhibition of vitronectin and fibrinogen binding to the vitronectin receptor and platelet glycoprotein IIb/IIIa are examined.

Strategy

The first investigations on the inhibition of fibrinogen and vitronectin binding to the $\alpha_V\beta_3$ and $\alpha_{IIb}\beta_3$ receptor led to the highly active and $\alpha_V\beta_3$ selective cyclic pentapeptide c(RGDfV),[30] which also suppresses tumor-induced angiogenesis in a chick chorioallantoic membrane model.[13] This peptide shows a βII′/γ-turn arrangement with D-Phe in the *i* + *1* position of the βII′-turn (Figure 1).[31] However, especially the conformation of the γ-turn is not well-defined, and this part of the backbone still shows a certain flexibility.[29b] Therefore, we wished to reduce the accessible conformational space by incorporation of several β-turn mimetics[32] (Figure 2). This restriction of flexibility should lead to a better insight into structure−activity relations. If the biologically active conformation is matched by these peptides, they should exhibit a tighter binding to the integrins for entropic reasons.[27]

The RGD sequence is very sensitive to modifications, and minor variations like the replacement of Gly with Ala lead to a drastic loss of activity.[33] Therefore, we replaced the D-Phe-

(13) (a) Brooks, P. C.; Montgomery, A. M. P.; Rosenfeld, M.; Reisfeld, R. A.; Hu, T.; Klier, G.; Cheresh, D. A. *Cell* **1994**, *79*, 1157−1164. (b) Friedlander, M.; Brooks, P. C.; Shaffer, R. W.; Kincaid, C. M.; Varner, J. A.; Cheresh, D. A. *Science* **1995**, *270*, 1500−1502.

(14) See refs 4−8.

(15) (a) Lee, J.-O.; Rieu, P.; Arnaout, M. A.; Liddington, R. C. *Cell* **1995**, *80*, 631−638. (b) Lee, J.-O.; Bankston, L. A.; Arnaout, M. A.; Liddington, R. C. *Structure* **1995**, *3*, 1333−1340.

(16) Wistow, G.; Turnell, B.; Summers, L.; Slingsby, C.; Moss, D.; Miller, L.; Lindley, P.; Blundell, T. J. *Mol. Biol.* **1983**, *107*, 175−202.

(17) Leahy, D. J.; Hendrickson, W. A.; Aukhil, I.; Erickson, H. P. *Science* **1992**, *258*, 987−991.

(18) (a) Acharya, R.; Fry, E.; Stuart, D.; Fox, G.; Rowlands, D.; Brown, F. *Nature* **1989**, *337*, 709−716. (b) Logan, D.; Abu-Ghazaleh, T.; Blakemore, W.; Curry, S.; Brown, F. *Nature* **1993**, *362*, 566−568.

(19) (a) Main, L. A.; Harvey, T. S.; Baron, M.; Boyd, J.; Campbell, I. D. *Cell* **1992**, *71*, 671−678. (b) Baron, M.; Main, L. A.; Driscoll, P. C.; Mardon, H. J.; Boyd, J.; Campbell, I. D. *Biochemistry* **1992**, *31*, 2068−2073.

(20) (a) Adler, M.; Lazarus, R. A.; Dennis, M. S.; Wagner, G. *Science* **1991**, *253*, 445−448. (b) Adler, M.; Carter, P.; Lazarus, R. A.; Wagner, G. *Biochemistry* **1993**, *32*, 282−289.

(21) (a) Dalvit, C.; Widmer, H.; Bovermann, G.; Breckenridge, R.; Metternich, R. *Eur. J. Biochem.* **1991**, *202*, 315−321. (b) Cooke, R. M.; Carter, B. G.; Martin, D. M. A.; Murray-Rust, P.; Weir, M. P. *Eur. J. Biochem.* **1991**, *202*, 323−328. (c) Saudek, V.; Atkinson, R. A.; Lepage, P.; Pelton, J. T. *Eur. J. Biochem.* **1991**, *202*, 329−338. (d) Saudek, V.; Atkinson, R. A.; Pelton, J. *Biochemistry* **1991**, *30*, 7369−7372. (e) Chen, Y.; Pitzenberger, S. M.; Grasky, V. M.; Lumma, P. K.; Sanyal, G.; Baum, J. *Biochemistry* **1991**, *30*, 11625−11636.

(22) Senn, H.; Klaus, W. *J. Mol. Biol.* **1993**, *232*, 907−925.

(23) Jeseja, M.; Smith, K. J.; Lu, X.; Williams, J. A.; Trayer, H.; Hyde, E. I. *Eur. J. Biochem.* **1993**, *218*, 853−860.

(24) Krezel, A. M.; Wagner, G.; Seymour-Ulmer, J.; Lazarus, R. A. *Science* **1994**, *264*, 1944−1947.

(25) (a) Müller, G.; Gurrath, M.; Kessler, H.; Timpl, R. *Angew. Chem. Int Ed. Engl.* **1992**, *31*, 326−328. (b) Kessler, H.; Diefenbach, B.; Finsinger, D.; Geyer, A.; Gurrath, M.; Goodman, S. L.; Hölzemann G.; Haubner, R.; Jonczyk, A.; Müller, G.; Graf von Roedern, E.; Wermuth, J. *Lett. Pept. Sci.* **1995**, *2*, 155−160.

(26) Dyson, H. J.; Rance, R. A.; Houghten, R. A.; Lerner, R. A.; Wright, P. E. *J. Mol. Biol.* **1988**, *201*, 161−200.

(27) Kessler, H. *Angew. Chem. Int. Ed. Engl.* **1982**, *21*, 512−523.

(28) (a) Hruby, V. *Life Sci.* **1982**, *31*, 189−199. (b) Gilon, C.; Halle, D.; Chorev, M.; Selinger, Z.; Byk, G. *Biopolymers* **1991**, *31*, 745−750.

(29) (a) See ref 25. (b) Mierke, D. F.; Kurz, M.; Kessler, H. *J. Am. Chem. Soc.* **1994**, *116*, 1042−1049. (c) Haubner, R.; Gratias, R.; Diefenbach, B.; Goodmann, S. L.; Joncyzk, A.; Kessler, H. *J. Am. Chem. Soc.*, in press.

(30) (a) Pfaff, M.; Tangemann, K.; Müller, B.; Gurrath, M.; Müller, G.; Kessler, H.; Timpl, R.; Engel, J. *J. Biol. Chem.* **1994**, *269*, 20233−2038. (b) Haubner, R.; Gurrath, M.; Müller, G.; Aumailly, M.; Kessler, H. In *Prospects in Diagnosis and Treatment of Breast Cancer, Excerpta Medica International Congress Series*; Schmitt, M., Greaff, H., Kindermann, G., Eds.; Elsevier Science Publishers: Amsterdam, The Netherlands, 1994; pp 133−144.

(31) (a) Aumailly, M.; Gurrath, M.; Müller, M.; Calvete, J.; Timpl, R.; Kessler, H. *FEBS Lett.* **1991**, *291*, 50−54. (b) Gurrath, M.; Müller, G.; Kessler, H.; Aumailly, M.; Timpl, R. *Eur. J. Biochem.* **1992**, *210*, 911−921.

(32) (a) Hölzeman, G. *Kontakte (Merck)* **1991**, *1*, 3−12. (b) Hölzeman, G. *Kontakte (Merck)* **1991**, *2*, 55−63.

(33) (a) Ali, F. E.; Calvo, R.; Romoff, T.; Samanen, J.; Nichols, A.; Store, B. in *Peptides: Chemistry, Structure and Biologie*; Rivier, J. E.; Marshall, G. R., Eds.; ESCOM Science Publishers B. V.: Leiden, The Netherlands, 1990; pp 94−96. (b) Nutt, R. F.; Brady, S. F.; Sisko, J. T.; Ciccarone, T. M.; Colton, C. D.; Levy, M. R.; Gould, R. J.; Zhang, G.; Freidman, P. A.; Veber, D. F. In *Peptides 1990: Procedings of the Twenty-First European Peptide Symposium*; Giralt, E., Andreu, D., Eds.; ESCOM Science Publishers B. V.: Leiden, The Netherlands, 1991; pp 784−786.

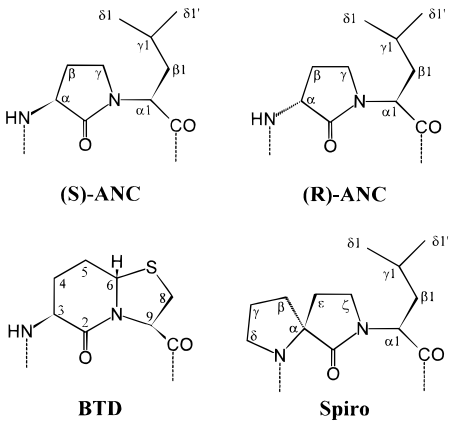

Figure 2. The different turn mimetics: (*S*)- and (*R*)-Gly[ANC-2]Leu dipeptide ((*S*)-ANC, (*R*)-ANC), β-turn dipeptide (BTD), and (*S*,*S*)-spiro-Pro-Leu moiety (spiro).

Val dipeptide by several different turn mimetics (see Figure 2) to fix the backbone conformation. The ability of the (*S*)- and (*R*)-Gly[ANC-2]Leu dipeptide[34] (*S*- and *R*-ANC) and the β-turn dipeptide[35] (BTD) as well as the (*S*,*S*)-spiro-Pro-Leu moiety[36] (spiro) to introduce turns in linear or cyclic peptides has already been demonstrated.[37] In our peptide analogues these building blocks should occupy the $i + 1$ and $i + 2$ position of the βII′-turn (Figure 1). The distinct turn mimetics thereby should reduce the flexibility of different backbone dihedral angles in the cyclic peptides. The ANC moiety fixes the ψ-angle of the amino acid in the $i + 1$ position of the β-turn. In contrast, the BTD and spiro motif fix one φ- and one ψ-angle (BTD: ψ_{i+1} and ϕ_{i+2}; spiro: ϕ_{i+1} and ψ_{i+1}). Therefore, the latter two turn mimetics should lead to more rigid cyclic peptides. Fixing the peptide in the region of the D-Phe-Val dipeptide should also influence the flexibility of the γ-turn on the opposite side.

To examine the influence of the ring size on the ability to induce a β-turn, the BTD moiety was also incorporated into the two cyclic pseudo-hexapeptides (c(RGD"BTD"V), **PA5**, and c(RaD"BTD"V), **PA6**). Cyclic hexapeptides normally adopt a conformation consistent of two opposed β-turns. It is known that a D-amino acid in such cyclic peptides induces a βII′-turn with the D-amino acid located in the $i + 1$ position.[38] We were interested to see whether the D-amino acid exhibits a higher preference to occupy the $i + 1$ position of the β-turn or if the turn motif forms the β-turn. Therefore, we chose, besides c(RGD"BTD"V), the biologically less interesting c(RaD"BTD"V) to investigate this aspect. For the latter compound two different conformations are possible: (a) the D-amino acid is dominant and induces a βII′-turn with D-Ala in $i + 1$ and the BTD moiety adopts a very unfavorable position at the side or (b) the turn mimetic occupies the $i + 1$ and $i + 2$ position of a βII′-turn, for which it is designed, and D-Ala is shifted in the $i + 2$ position of the adverse second turn.

Experimental Methods

Synthesis of the Turn Mimetics. Synthesis of the BTD (Figure 2) follows the scheme outlined by Bach et al.[37e] However, it was modified concerning the protecting group strategy and deprotection route. We wanted to introduce the BTD moiety using solid phase peptide synthesis with 9-fluorenylmethoxycarbonyl (Fmoc) strategy. Thus, the N-terminal Boc-protecting group had to be exchanged by the Fmoc group. The deprotection of the phthaloyl group with hydrazine in the presence of the C-terminal ethyl ester results in the C-terminal hydrazide in high amounts. Therefore, the ethyl ester was cleaved first under acidic conditions using a 4:1 mixture of acetic acid and concentrated hydrochloric acid. The phthaloyl group was unaffected under these conditions, leading to Pht-BTD-OH. Subsequent hydrazinolysis of the phthaloyl group and reprotection of the N-terminus gave the desired Fmoc-BTD-OH.

Gly[ANC-2]Leu building blocks (Figure 2) were synthesized according to the literature.[34,39] The Boc-protecting group was exchanged similarly as described.[39] The Fmoc-protected (*S*,*S*)-4,4-spirolactam moiety (Fmoc-(*S*,*S*)-spiro-Pro-Leu-OH, Figure 2) was purchased from Neosystems, France.

Synthesis of the Peptide Analogues. Linear peptides were assembled leaving the glycine residue at the C-terminus to prevent racemization and steric hindrance during the cyclization step. The synthesis was performed using Merrifield solid phase peptide synthesis[40] with Tentagel[41] (peptides **PA1**, **PA2**, and **PA4**) or *o*-chlorotritylchlorid[42] (cTrt) resins (peptides **PA3**, **PA5**, and **PA6**) applying Fmoc-strategy.[43] The Fmoc-protected amino acids and turn mimetics were coupled with *O*-(1*H*-benzotriazol-1-yl)-*N*,*N*,*N*′,*N*′-tetramethyluronium tetrafluoroborate (TBTU) and 1-hydroxybenzotriazole (HOBt) using diisopropylethylamine (DIEA) as base. The Fmoc group was cleaved with 20% piperidine in dimethylformamide (DMF). Peptides were cleaved from the cTrt solid support by acetic acid/2,2,2-trifluoroethanol(TFE)/dichlormethane (1:1:3) or from the Tentagel solid support by hydrogenation. Both procedures lead to peptides with intact side chain protecting groups. Cyclization was performed via *in situ* activation using diphenyl phosphorazidate (DPPA) in DMF with sodium bicarbonate as a solid base[44] or *N*-ethyl-*N*,*N*′-(dimethylaminopropyl)-carbodiimide (EDCI) and 4-(*N*,*N*-dimethylamino)pyridine (DMAP) under high dilution conditions. Final deprotection was done with trifluoracetic acid (TFA) and scavengers.

Purification by reverse phase high-performance liquid chromatography (RP-HPLC) yielded peptide analogues, which were >95% pure. All peptides were characterized by fast atom bombardment (FAB) mass spectrometry and various NMR techniques (for data see supporting information).

NMR Spectroscopy. All spectra were recorded in DMSO-d_6 solution and calibration was performed with reference to the residual DMSO signal (^1H, 2.49 ppm; ^{13}C, 39.5 ppm). The assignment of all proton and carbon resonances followed the standard strategy as previously described.[45] Sequential assignment was accomplished by through-bond connectivities from heteronuclear multibond correlation

(34) (a) Freidinger, R. M., Veber, D. F.; Perlow, D. S.; Brooks, J. R.; Saperstein, R. *Science* **1980**, *210*, 656−658. (b) Freidinger, R. M.; Schwenk Perlow, D. S.; Veber, D. F. *J. Org. Chem.* **1982**, *47*, 104−109.

(35) (a) Nagai, U.; Sato, K. *Tetrahedron Lett.* **1985**, *26*, 647−650. (b) Nagai, U.; Sato, K. In *Peptides: Structure and Function. Proceedings of the 9th American Peptide Symposium*; Veber, C. M., Hruby, V. J., Kopple, K. D., Eds.; Pierce Chemical Co.: Rockford, Illinois, 1985; pp 465−468.

(36) (a) Hinds, M.G.; Richards, N. G.; Robinson, J. A. *J. Chem. Soc. Chem. Commun.* **1988**, 1447−1449. (b) Genin, M. J.; Gleason, W. B.; Johnson, R. L. *J. Org. Chem.* **1993**, *58*, 860−866.

(37) (a) Nagai, U.; Kato, R.; Sato, K.; Ling, N.; Matsuzaki, T.; Tomotake, Y. In *Peptides: Chemistry and Biology. Proceedings of the 10th American Peptide Symposium*; Marshall, G. R., Ed.; ESCOM Science Publishers B. V.: Leiden, The Netherlands, 1988; 129−130. (b) Williams, B. J.; Curtis, N. R.; McKnight, A. T.; Maguire, J.; Foster, A.; Tridgett, R. *Reg. Pept.* **1988**, *22*, 189. (c) Ward, P.; Ewan, G. B.; Jordan, C. C.; Ireland, S. J.; Hagan, R. M.; Brown, J. R. *J. Med. Chem.* **1990**, *33*, 1848−1851. (d) Hinds, M. G.; Welsh, J. H.; Brennand, D. M.; Fisher, J.; Glennie, M. J.; Richards, N. G. J.; Turner, D. L.; Robinson, J. A. *J. Med. Chem.* **1991**, *34*, 1777−1789. (e) Bach, A. C., II; Markwalder, J. A., Ripka, W. C. *Int. J. Pept. Protein Res.* **1991**, *38*, 314−323.

(38) Kessler, H. In *Trends in Drug Research*; Claasen, V., Ed.; Elsevier Science Publishers: Amsterdam, 1990; pp 73−84.

(39) Williams, B. J.; Curtis, N. R.; McKnight, A. T.; Maguire, J. J.; Young, S. C.; Veber, D. F.; Baker, R. *J. Med. Chem.* **1993**, *36*, 2−10.

(40) (a) Merrifield, R. B. *J. Am. Chem. Soc.* **1963**, *85*, 2149−2154. (b) Merrifield, R. B. *Angew. Chem.* **1985**, *97*, 801−812.

(41) Rapp, W.; Fritz, H.; Bayer, E. In *Peptides: Chemistry and Biology*; Smith, J. A.; Rivier, J. E., Eds.; ESCOM Science Publishers B. V.: Leiden, The Netherlands, 1992; pp 529−530.

(42) (a) Barlos, K.; Gatos, D.; Kallitsis, J.; Papahotiu, G.; Sotiriu, P.; Wenqing, Y.; Schäfer, W. *Tetrahedron Lett.* **1989**, *30*, 3943−3946. (b) Barlos, K.; Chatzi, O.; Gatos, D.; Stavropoulos, G. *Int. J. Pept. Protein Res.* **1991**, *37*, 513−520.

(43) Fields, G. B.; Noble, R. L. *Int. J. Pept. Protein Res.* **1990**, *35*, 161−214.

(44) Brady, S. F.; Paleveda, W. J.; Arison, B. H.; Freidinger, R. M.; Nutt, R. F.; Veber, D. F. In *Peptides: Structure and Function. Proceedings of the 8th American Peptide Symposium*; Hruby, V. J., Rich, D. H., Eds.; Pierce Chemical Co.: Rockford, Illinois, 1983; pp 127−130.

Table 1. Temperature Dependence of the Amide Proton Chemical Shift of the Peptide Analogues in DMSO[a].

		amino acid				
no.	peptide analogue	Arg^1	Gly^2/D-Ala^2	Asp^3	$Mim^{4\,b}$	Val^5
PA1	c(RGD"*S*-ANC")	−0.5	−6.3	−7.3	−1.1	
PA2	c(RGD"*R*-ANC")	−2.3	−2.3	−7.3	−0.9	
PA3	c(RGD"BTD")	1.1	−6.0	−9.7	3.0	
PA4	c(RGD"spiro")	−2.6	−9.3	−2.8		
PA5	c(RGD"BTD"V)	−4.7	−6.7	−3.4	−6.8	−0.7
PA6	c(RaD"BTD"V)	−3.7	−6.7	−4.4	−5.1	−0.9

[a] The coefficients are given in parts per billion per K. [b] Corresponding turn mimetic.

(HMBC)[46] spectra. Aromatic and carbonyl resonances were also assigned using through bond long-range correlations. As only one set of signals for each peptide could be detected, no cis−trans isomerization at peptide bonds occurs under measurement conditions. Proton distances were calculated according to the isolated two-spin approximation from volume integrals of nuclear Overhauser enhancement (NOESY)[47] or rotating frame nuclear Overhauser enhancement (ROESY)[48] spectra. NOESY spectra were recorded with mixing times of 150 ms (for **PA1** and **PA3**) and compensated ROESY spectra with 200 ms (for **PA2**, **PA4**, **PA5**, and **PA6**). Homonuclear coupling constants have been measured from one-dimensional spectra and from P.E.COSY[49] crosspeaks. Determination of the heteronuclear vicinal coupling constants followed the scheme of Titman and Keeler from a combination of HMBC spectra with *z*-filtered TOCSY.[50] For peptide analogues **PA5** and **PA6** $^3J(H^N,C^\beta)$ coupling constants were extracted from HETLOC experiments.[51] Temperature coefficients for the amide protons of each peptide were determined via one-dimensional spectra in the range from 300 to 340 K with a step size of 5 K (Table 1). Chemical shift data, proton distances and determined coupling constants are listed in the supporting information.

Computational Methods. A two-step method for the prediction of the conformations was applied: a restrained distance geometry (DG) calculation to explore the conformational space of the peptides, followed by a restrained molecular dynamic (MD) simulation using explicit solvent for the refinement of the structures. Upper and lower bounds for proton distances were generated by adding or subtracting 10% of the experimental NOE and ROE value. Coupling constants were used directly as restraints.[52]

Distance geometry calculations were performed using the Disgeo program.[53] For each peptide 100 structures have been embedded into the four-dimensional space using the random metric matrix algorithm.[54] The optimization step consists of 200-step steepest-descent minimization followed by a short distance driven dynamic (DDD) run (5 ps with a strong coupling to a temperature bath at 300 K and 2 ps with a weak coupling to 1 K) using NOEs as restraints. After reprojection into the three-dimensional space, 200 steps of steepest-descent minimization to optimize the chiral volumes were performed. Final optimization was achieved with a two-step distance-, and angle-driven dynamic (DADD)[55] simulation (5 ps with a strong coupling to a temperature bath of 500 K and 2 ps with a weak coupling to 1 K) using NOEs, vicinal coupling constants, and chiral volumes. The resulting structures for each peptide were analyzed for convergence. RMSD values for the superposition of the backbone C′, N, and C^α atoms were in the range of 4 to 38 pm for each compound; therefore, the structure with the lowest total error was used as a starting structure for a subsequent MD simulation using a modified version of the Gromos program.[56] The structures were placed in a truncated octahedron which was filled with DMSO molecules.[57] This box was then energy minimized in two steps (each with 2000 steps of steepest descent), the first one to relax the solvent molecules while the peptide is held fixed and the second for all atoms. A MD trajectory was recorded for 170 ps at a temperature of 300 K using NOEs and coupling constants as restraints (k_{NOE} = 2000 kJ/(mol nm^2); k_J = 1 kJ/(mol rad^2)) and each picosecond a structure was stored. The first 70 ps of the individual trajectories were disregarded to account for equilibration, the last 100 ps were analyzed for violation of experimental data, population of hydrogen bonds, and dihedral transitions. The structures presented in this paper have been averaged over the last 100 ps of the MD run and minimized by 200 steps of steepest descent.

Results

Structures of the Cyclic Pentapeptides. c(RGD"*S*-ANC"), PA1. The structure of **PA1** as determined in DMSO does not exhibit the expected conformation. Gly occupies the *i + 1* position of a distorted βII′-turn while the *S*-ANC moiety is located in the *i + 3* and *i + 4* position. The conformation of the β-turn is slightly distorted, the particular hydrogen bond is not populated throughout the whole MD simulation. The amide protons of Arg^1 and of the turn mimetic show the smallest temperature dependence of chemical shifts since Arg^1-H^N is sterically shielded from the solvent and ANC^4-H^N is involved in the hydrogen bond of the βII′-turn. The assignment of the diastereotopic β-protons of Asp^3 was achieved using the $^3J(H^\alpha,H^\beta)$ coupling constants in combination with the H^N,H^β and H^α,H^β proton distances. Subsequently, the population of the side chain rotamers of Asp^3 can be calculated from the homonuclear H^α,H^β coupling constants according to the Pachler equations.[58] The gauche (−) rotamer ($\chi_1 = -60°$) is predominant with a value of 56%. In contrast, the side chain of Arg^1 is flexible, its orientation as shown in Figure 3 is arbitrarily.

c(RGD"*R*-ANC"), PA2. The peptide **PA2** exhibits a higher flexibility in DMSO than **PA1** and shows a lower tendency to occupy a predominant conformation. The β-turn with Gly^2 in the *i + 1* position, as found for the peptides **PA1** and **PA3**, is populated only to a degree of 12%. The carbonyl oxygen of Arg^1 is also involved in a γ-turn (bifurcation), as is common in βII′-turns. The structural element with the highest invariability is a γ-turn with *R*-ANC in the *i* and *i + 1* position (populated

(45) (a) Kessler, H.; Seip, S. in *Two-Dimensional NMR-Spectroscopy; Applications for Chemists and Biochemists*; Croasmun, W. R., Carlson, M. K., Eds.; VCH Puplishers: New York, 1994; pp 619−654. (b) Kessler, H.; Schmitt, W. in *Encyclopedia of Nuclear Magnetic Resonance*; Grant, D. M., Harris, R. K., Eds.; J. Wiley & Sons: New York, 1995; in press.

(46) (a) Bax, A.; Summers, M. T. *J. Am. Chem. Soc.* **1986**, *108*, 2093−2094. (b) Bermel, W.; Wagner, K.; Griesinger, C. *J. Magn. Reson.* **1989**, *83*, 223−232. (c) Emsley, L.; Bodenhausen, G. *J. Magn. Reson.* **1989**, *82*, 211−221. (d) Kessler, H.; Schmieder, P.; Köck, M.; Kurz, M. *J. Magn. Reson.* **1990**, *88*, 615−618.

(47) (a) Jeener, J.; Meier, B. H.; Bachmann, P.; Ernst, R. R. *J. Chem. Phys.* **1979**, *71*, 4546−4553. (b) Wüthrich, K. In *NMR of Proteins and Nucleic Acids*; Wiley & Sons: New York, 1986.

(48) (a) Bothner-By, A. A.; Stephensen, R. L.; Lee, J.; Warren, C. D.; Jeanloz, R. W. *J. Am. Chem. Soc.* **1984**, *106*, 811−813. (b) Kessler, H.; Griesinger, C.; Kerssebaum, R.; Wagner, K.; Ernst, R. R. *J. Am. Chem. Soc.* **1987**, *109*, 607−609.

(49) Mueller, L. *J. Magn. Reson.* **1987**, *72*, 191−196.

(50) (a) Titman, J. J.; Neuhaus, D.; Keeler, J. *J. Magn. Reson.* **1989**, *85*, 111−131. (b) Titman, J. J.; Keeler, J. *J. Magn. Reson.* **1990**, *89*, 640−646.

(51) Kurz, M.; Schmieder, P.; Kessler, H. *Angew. Chem. Int. Ed. Engl.* **1991**, *30*, 1329−1330.

(52) (a) Kim, Y.; Prestegard, J. H. *Proteins: Struct. Funct. Genet.* **1990**, *8*, 377−382. (b) Mierke, D. F.; Kessler, H. *Biopolymers* **1992**, *32*, 1277−1282. (c) Eberstadt, M.; Mierke, D. F.; Köck, M.; Kessler, H. *Helv. Chim. Acta* **1992**, *75*, 2583−2592.

(53) (a) Havel, T. F.; Wüthrich, K. *Bull. Math. Biol.* **1984**, *46*, 673−698. (b) Havel, T. F. DISGEO, Quantum Chemistry Exchange Program, Exchange No. 507, Indiana University, 1988. (c) Crippen, G. M.; Havel, T. F. Distance Geometry and Molecular Conformation; Research Studies Press LTD., John Wiley & Sons: Somerset, England, 1988. (d) Havel, T. F. *Prog. Biophys. Mol. Biol.* **1991**, *56*, 43−78.

(54) (a) Havel, T. F. *Biopolymers* **1990**, *29*, 1565−1585. (b) Reference 53d.

(55) Mierke, D. F.; Kessler, H. *Biopolymers* **1993**, *33*, 1003−1017.

(56) (a) Hermans, J.; Berendsen, H. J. C.; Van Gunsteren, W. F.; Postma, J. P. M. *Biopolymers* **1984**, *23*, 513−1518. (b) van Gunsteren, W. F.; Berendsen, H. J. C. Groningen Molecular Simulations (GROMOS) Library Manual. *GROMOS user manual*; Biomos B. V.: Nijenborgh 16 NL 9747 AG Groningen, 1987. (c) van Gunsteren, W. F.; Berendsen, H. J. C. *Angew. Chem. Int. Ed. Engl.* **1990**, *29*, 902−1023.

(57) Mierke, D. F.; Kessler, H. *J. Am. Chem. Soc.* **1991**, *113*, 9466−9470.

(58) (a) Pachler, K. G. R. *Spectrochim. Acta* **1963**, *19*, 2085−2092. (b) Pachler, K. G. R. *Spectrochim Acta* **1964**, *20*, 581−587.

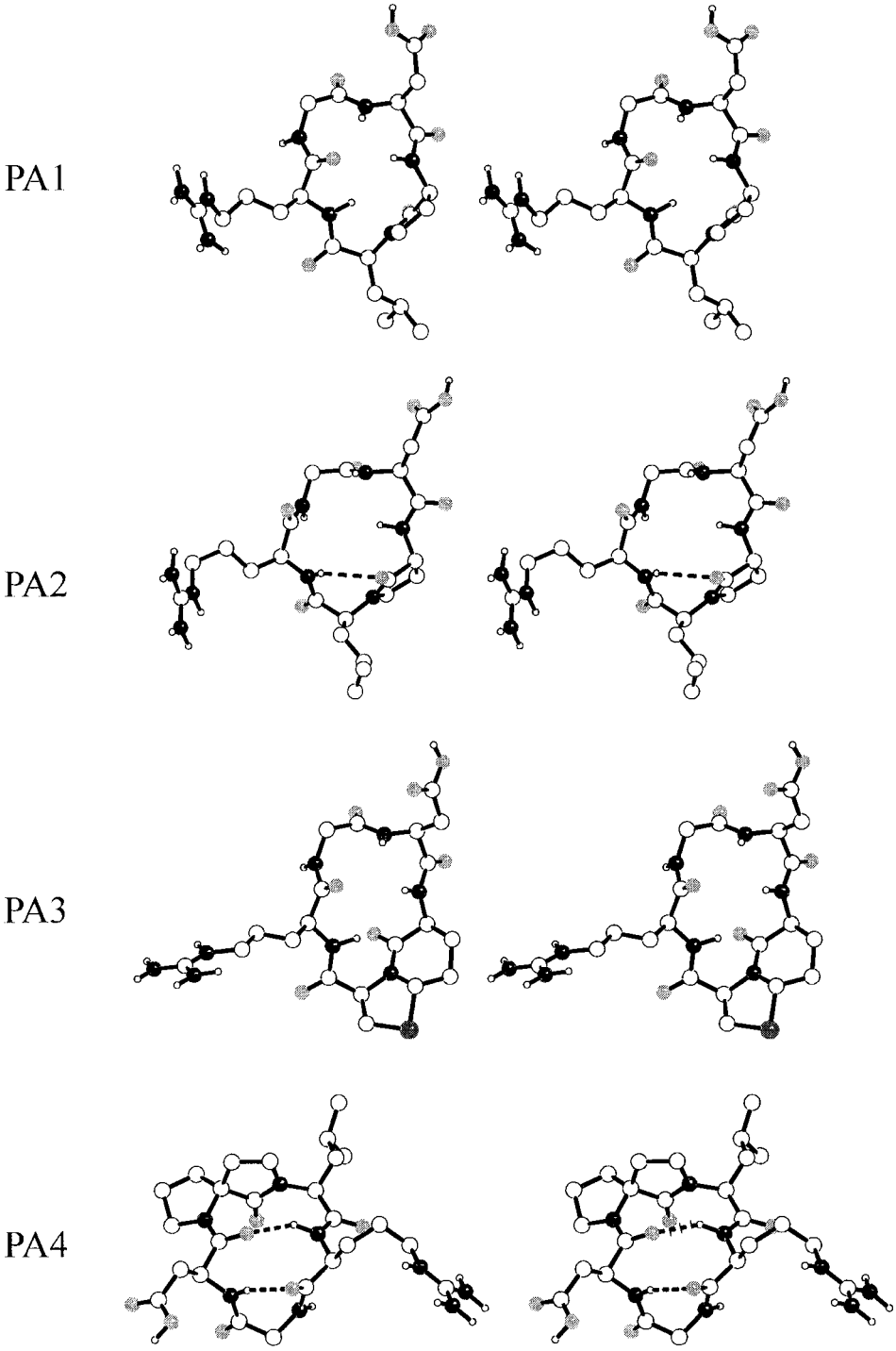

Figure 3. Stereoplots of the averaged and energy-minimized conformations of c(RGD"*S*-ANC") (**PA1**), c(RGD"*R*-ANC") (**PA2**), c(RGD"BTD") (**PA3**), and c(RGD"spiro") (**PA4**) resulting from restrained MD simulations in DMSO. Carbon and hydrogen atoms are white; nitrogen atoms are black; oxygen atoms are gray; the sulfur atom of **PA3** is dark gray.

to 98%). Another dominating structural feature is an inverse γ-turn with Asp^3 in the $i + 1$ position, which is found in half of the structures during the MD simulation. As indicated by the homonuclear $^3J(H^\alpha,H^\beta)$ coupling constants (7.6 and 6.5 Hz), the side chain of Asp^3 shows no predominant orientation.

c(RGD"BTD"), PA3. Analogous to the structure of **PA1** in solution, Gly^2 adopts the $i + 1$ position of a distorted βII′-turn and the BTD moiety is located in the $i + 3$ and $i + 4$ positions, respectively. The RMSD value for the superposition of the backbone C$^\alpha$, C′, and N atoms of **PA1** and **PA3** is only 33 pm. The experimental data were reproduced very well. Only the $^3J(H^N,H^\alpha)$ and the $^3J(H^N,C')$ coupling constants of Arg^1 calculated from the ϕ-angle of the averaged and minimized structure deviate more. During the restrained dynamic simulation this dihedral angel fluctuates between the extreme values of $-150°$ and $+110°$. The coupling constants averaged over the whole trajectory are much closer to the experimental values than those calculated from the averaged and minimized structure. The small temperature coefficient of the amide proton of Arg^1 can be explained by the internal orientation and the resulting sterical shielding from the solvent. The second amide proton with a small temperature dependence is the BTD-H^N, which is involved in the hydrogen-bond forming the β-turn. The orientation of the Asp^3 side chain ($\chi_1 = -60°$ populated to 61%) is similar to that of **PA1** and Arg^1 is flexible.

c(RGD"spiro"), PA4. The (*S*,*S*)-spiro-Pro-Leu moiety adopts the desired $i + 1$ and $i + 2$ position of a βII′-turn and Gly^2 is in the $i + 1$ position of a γ-turn at the opposite side of the

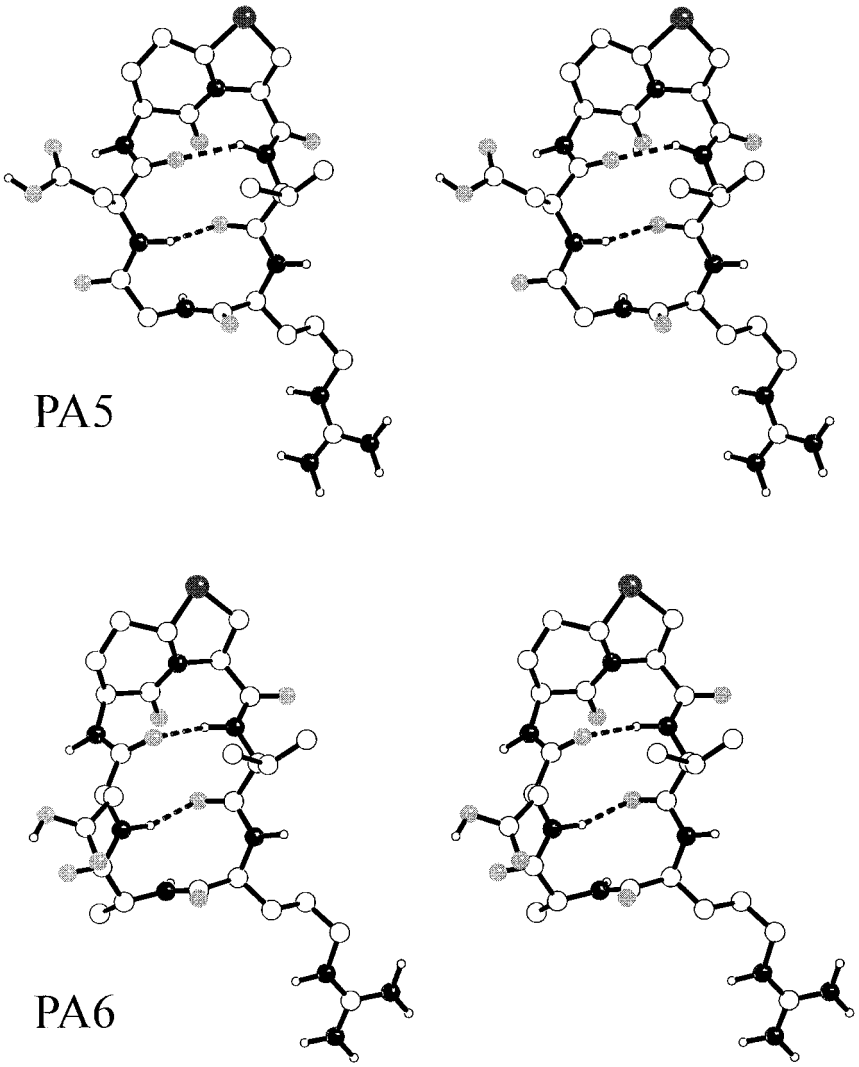

Figure 4. Stereoplots of the averaged and energy minimized conformations of c(RGD"BTD"V) (**PA5**) and c(RaD"BTD"V) (**PA6**) resulting from restrained MD simulations in DMSO. Carbon and hydrogen atoms are white; nitrogen atoms are black; oxygen atoms are gray; sulfur atoms are dark gray.

molecule. Both hydrogen bonds are populated throughout the whole MD simulation. Chemical shifts of the particular amide protons show only a small temperature dependence (Table 1). The homonuclear $^3J(H^\alpha,H^\beta)$ coupling constants of Arg[1] (8.0 and 6.3 Hz) reflect the population of more than one conformation of this side chain. Both other side chains (Asp[3] and the isobutyl side chain of the spiro moiety) adopt a rotamer with a value of $-60°$ for the χ_1-angle. This rotamer of Asp[3] is populated to a degree of 62%. Due to the hydrophobic interaction of the δ_1-methyl groups with the neighboring ϵ- and ζ-methylene groups within the spiro moiety, the population of this side chain rotamer is much higher (88%). The conformation of this cyclic peptide seems to be quite rigid as all experimental data are well-fulfilled by the averaged and minimized structure.

Structures of the Cyclic Hexapeptides. c(RGD"BTD"V), PA5, and c(RaD"BTD"V), PA6. The structures of both peptides show a similar β/β-conformation, which is typical for cyclic hexapeptides. BTD adopts the $i + 1$ and $i + 2$ position of a βII′-turn, and Gly[2] or D-Ala[2] are located in the $i + 2$ position of a βII-turn on the opposite side. In both compounds the amide proton of Val[5] shows the smallest temperature coefficient, corresponding to a highly populated hydrogen bond. The larger temperature coefficient of both Asp[3]-H^N indicates that the corresponding turn is less rigid. The side chain of Arg[1] is freely rotating in both compounds. In **PA6** the H^β protons of Asp[3] are degenerated, indicating a flexible side chain, while in **PA5** an orientation with a χ_1-angle of $-60°$ is dominating (populated to 63%).

Biological Data. The inhibitory capacities of the peptide analogues on the binding of vitronectin and fibrinogen to the isolated, immobilized $\alpha_{IIb}\beta_3$- and $\alpha_V\beta_3$-receptors were compared with the activity of the c(RGDfV) and the linear standard peptide GRGDSPK. Peptide analogues **PA4** and **PA6** show no activity for either receptor. Peptide analogues **PA1**, **PA2**, **PA3**, and **PA5** show an increased activity compared to the linear standard peptide GRGDSPK with respect to the inhibition of vitronectin binding to the $\alpha_V\beta_3$-receptor. Only compound **PA2** has a higher inhibitory activity on vitronectin binding than the lead structure c(RGDfV).

In contrast, peptide derivatives **PA2** and **PA5** reveal an increased activity and compounds **PA1** and **PA3** a decreased activity compared to GRGDSPK concerning the inhibition of fibrinogen binding to the $\alpha_{IIb}\beta_3$-receptor. Similar to the effects on the $\alpha_V\beta_3$-receptor, compound **PA2** reveals a 10-fold higher activity than the lead peptide c(RGDfV). Thus **PA2** is the derivative with the highest activities among all compounds of this series, but possesses only little selectivity (10-fold higher activity for inhibition of vitronectin binding to $\alpha_V\beta_3$ than for fibrinogen binding to $\alpha_{IIb}\beta_3$). On the contrary, peptide analogue **PA1** is 10-fold less active in inhibiting vitronectin binding to the $\alpha_V\beta_3$-receptor compared to c(RGDfV), but shows a 100-fold higher inhibitory activity for vitronectin binding to $\alpha_V\beta_3$

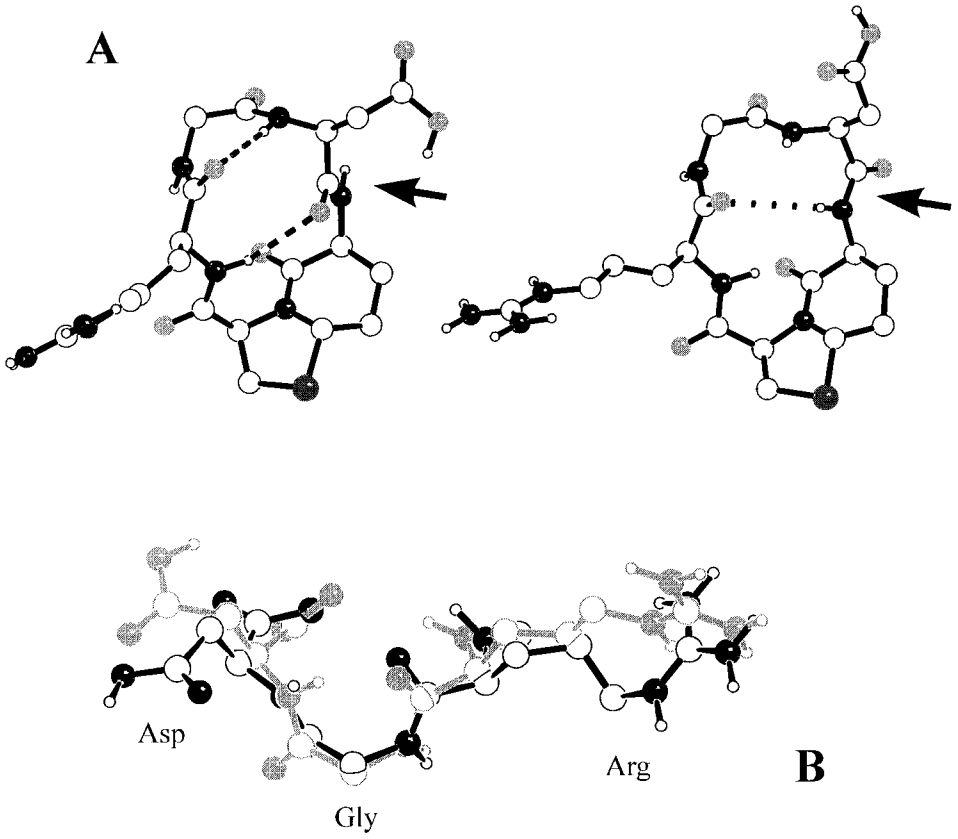

Figure 5. (A) Expected (left) and calculated (right) conformation of **PA3**. The characteristic difference of both conformations is focused on the orientation of the amide bond between Asp[3] and BTD[4]. (B) Superimposing of the RGD site of c(RGDfV) (gray) and c(RGD"BTD") **PA3** (black).

than for fibrinogen binding to $\alpha_{IIb}\beta_3$ and is thus the most selective compound in this series.

According to these results the peptide derivatives can be divided into four categories concerning the inhibition of vitronectin binding to the $\alpha_V\beta_3$-receptor: (a) very active, but less selective, c(RGD"*R*-ANC") (**PA2**); (b) active and selective, c(RGD"*S*-ANC") (**PA1**); (c) active and less selective, c(RGD"BTD") (**PA3**) and c(RGD"BTD"V) (**PA5**); (d) not active, c(RGD"spiro") (**PA4**) and c(RaD"BTD"V) (**PA6**).

Discussion

Structural Aspects. Our results demonstrate that the BTD moiety is not able to induce a β-turn at the desired position in **PA3**. Glycine, which also prefers to adopt the *i + 1* position in β- or γ-turns, is part of the detected β-turn. The major difference between the expected and the resulting structure is the orientation of the amide plane adjacent to Asp[3] (Figure 5). As both accompanying C^α-atoms have the *S*-configuration, the orientation found in DMSO may be caused by minimization of gauche interactions as well as 1,3-allylic strain. The peptide carbonyl oxygen has a strong tendency to be orientated parallel to the C−H bond at the α-carbon atom of the following amino acid (here BTD). Although the backbone structure differs from that initially designed, the conformation of the important RGD-binding site is similar to that in the lead compound c(RGDfV). This is shown in the superposition of the RGD pharmacophore of both structures in Figure 5.

A comparison of **PA1** with the structure of the other diastereomer **PA2** shows only minor variations of the backbone conformation (Figure 3 and 6). Both peptides possess a β-turn with Gly[2] in the *i + 1* position. The most remarkable difference is the orientation of the lactam bond of the ANC moiety. The *S*-ANC differs from the *R*-ANC derivative by a 180° rotation of this lactam bond. Thus the carbonyl group of the *R*-ANC motif forms a hydrogen bond in a γ-turn, and the carbonyl group

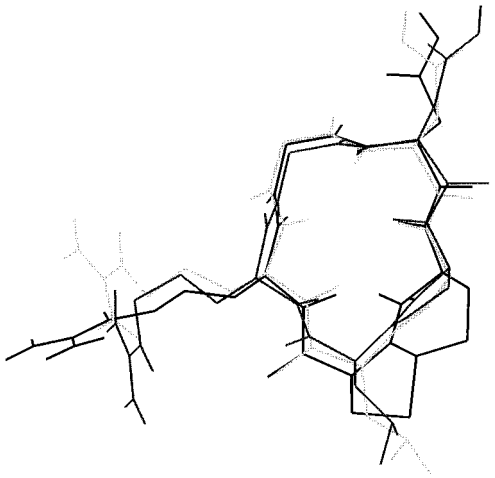

Figure 6. The superimposing of **PA1** (light gray), **PA2** (gray) and **PA3** (black) show that the conformation of the RGD site is very similar in all three peptides.

of the *S*-ANC motif is orientated antiparallel to the corresponding amide hydrogen. In addition, the value of the Gly[2] φ-angle deviates about 40° in both structures.

An analysis of the dihedral angles in the *i + 3* and *i + 4* position of ten cyclic RGD pentapeptides from our group[59] which possess a βII′/γ-turn structure reveals angles of −140° ± 20° (ϕ_{i+3}), +100° ± 20° (ψ_{i+3}), 80° ± 15° (ϕ_{i+4}) and −60° ± 15° (ψ_{i+4}). The ANC moieties of **PA1** and **PA2** fix only one ψ-angle of the backbone. This angle can achieve values in the range of −140° ± 10° (**PA1**) or 140° ± 10° (**PA2**).[37c] A comparison with the ψ_{i+3}-angle in an ideal βII′/γ-conformation (see above) shows that the *R*-ANC moiety fits also in this position. In contrast, the *S*-ANC moiety is not suitable for an

(59) See refs 29c and 31.

Table 2. Inhibition of Fibrinogen (Fbg) Binding to the $\alpha_{IIb}\beta_3$-Receptor and Vitronectin (Vn) Binding to the $\alpha_V\beta_3$-Receptor[a]

		$\alpha_{IIb\beta3}$ (Fbg)		$\alpha_{V\beta3}$ (Vn)	
no.	peptide analogue	IC_{50} (μM)	*Q*	IC_{50} (μM)	*Q*
	GRGDSPK		1		1
	c(RGDfV)	8.3×10^{-1}	5.0	2.2×10^{-3}	6.1×10^{-3}
PA1	c(RGD"*S*-ANC")	2.8	1.6	4.0×10^{-2}	1.1×10^{-2}
PA2	c(RGD"*R*-ANC")	8.5×10^{-3}	4.9×10^{-3}	8.5×10^{-4}	2.3×10^{-4}
PA3	c(RGD"BTD")	4.8	2.7	2.8×10^{-1}	7.3×10^{-2}
PA4	c(RGD"spiro")	na[b]		na	
PA5	c(RGD"BTD"V)	5.5×10^{-1}	3.1×10^{-1}	4.3×10^{-2}	1.1×10^{-2}
PA6	c(RaD"BTD"V)	na		na	

[a] Values are given as IC_{50} and as quotients $Q = IC_{50}$[peptide]/IC_{50}[GRGDSPK]. [b] na, not active.

ideal βII′/γ-conformation. A MD simulation in vacuo for 1 ns for the BTD building block shows that the two restricted dihedrals can reach values of $-130° \pm 50°$ (ψ) and $-90° \pm 40°$ (ϕ'). We interpret our structural results as a balance between the high steric strain in these cyclic pentapeptides and the geometric restriction of the particular dihedral angles in the corresponding turn mimetics. It seems as if the location of the incorporated building blocks in the βII′-turn leads to an unfavorable strain in our cyclic pentapeptides. Therefore, *R*-ANC prefers the relative *i* + *3* and *i* + *4* position which also fits the restricted ψ-angle. It has been shown that cyclic pentapeptides are still quite flexible in the region of the γ-turn.[29a] For that reason the adaptation of the *S*-ANC and the BTD moiety in the *i* + *3* and *i* + *4* position might be energetically favored over a location in a β-turn, although the particular dihedral angles do not fit the ideal values. The spiro moiety in **PA4** fixes the two consecutive dihedral angles ϕ ($+75° \pm 20°$) and ψ ($-140° \pm 10°$).[37c] One of these two fixed angles is the ϕ-angle in the *i* + *1* position. If the turn mimetic would occupy the *i* + *3* and *i* + *4* position, not only the flexible γ-turn but also the more rigid β-turn would be strongly distorted. Therefore, **PA4** prefers the desired βII′/γ-conformation in solution.

To test whether the BTD building block is able to induce turns in cyclic peptides at all, two cyclic hexapeptides were synthesized. To incorporate a turn mimetic into the sequence of the lead compound c(RGDfV), two principal possibilities exist: the substitution of either Phe or Val. The structure of c(RGDF"BTD") has already been described by Hann et al.[60] This compound shows a conformation consistent with two facing β-turns, where BTD adopts the *i* + *1* and *i* + *2* positions of one turn and Gly^2 is in *i* + *1* position at the opposite side. This is the conformation one would expect for such a molecule because the relative orientation of the turn mimetic and of the Gly residue fits to their preferred positions in the reverse turns. D-Amino acids and Gly exhibit a high tendency to occupy the *i* + *1* position of β-turns.[38] The sequences of **PA5**, and **PA6** do not allow that the BTD moiety and Gly^2 or D-Ala^2, respectively, occupy their preferred positions in two facing turns simultaneously. The calculated structures of both cyclic hexapeptides show one βII′-turn with the BTD building block in the *i* + *1* and *i* + *2* position and Gly^2 or D-Ala^2 in the *i* + *2* position of a facing βII-turn. These results lead to the conclusion that, in these cyclic hexapeptides, the turn-inducing potential of BTD exceeds that of Gly^2 and D-Ala^2, respectively. The strain in cyclic hexapeptides is not as high as in cyclic pentapeptides. A comparison with the backbone dihedral angles found for cyclic hexapeptides having a βII′/β-conformation[31] shows that for the BTD building block only one location in the turn is possible. The position at the side of the turn (*i* + *3* and *i* + *4*) is excluded by the restricted dihedral angles.

Structure−Activity Relationship. In **PA1**, **PA2**, and **PA3** the region of the biological relevant RGD sequence has a very similar conformation (Figure 6). All three analogues show a slightly distorted βII′-turn arrangement with Gly^2 in the *i* + *1* position. These β-turn arrangements correspond with the structures found for a group of active peptides with the sequence c(RGDFx). In these peptides Gly^2 also adopts the *i* + *1* position of a βII′-turn.[29c] The analysis of the parameters determining the relative orientation of the pharmacophoric groups (Arg and Asp side chain) also shows that the $ArgC^\alpha/AspC^\alpha$ and the $ArgC^\beta/AspC^\beta$ distances as well as the μ(Arg)-, ν(Asp)-, and φ-angle (for definition see Table 3 and ref 61) are very similar and correspond with the data found for the peptides with the sequence c(RGDFx) (Table 3).

Table 3. Characterization of the Relative Orientation of the Biologically Relevant RGD Sequence

no.	peptide analogue	C^α/C^α	C^β/C^β	μ(Arg)[c]	ν(Asp)[d]	φ[e]
PA1	c(RGD"*S*-ANC")	562	781	140	132	4
PA2	c(RGD"*R*-ANC")	618	850	152	127	−5
PA3	c(RGD"BTD")	589	783	137	123	10
PA4	c(RGD"spiro")	530	670	119	118	−11
PA5	c(RGD"BTD"V)	576	815	165	123	56
PA6	c(RaD"BTD"V)	539	706	151	101	29
	c(RGDfV)	547	668	113	113	−6
	c(RGDFk)	605	840	150	132	13

[a] Distance between the C^α atoms of Arg^1 and Asp^3, in pm. [b] Distance between the C^β atoms of Arg^1 and Asp^3, in pm. [c] Angle formed by the $C^\beta-C^\alpha$(Arg) vector and the C^α(Arg)$-C^\alpha$(Asp) vector, in deg. [d] Angle formed by the $C^\beta-C^\alpha$(Asp) vector and the C^α(Asp)$-C^\alpha$(Arg) vector, in deg. [e] Dihedral formed by the $C^\alpha-C^\beta$ vectors of Arg and Asp, in deg.

Despite these structural similarities at the RGD site, the peptide analogues reveal very different biological activities. The activity increases in the series **PA3** < **PA1** < **PA2** (Table 2).

There are two possible explanations: (a) structural differences in the region flanking the RGD sequence or (b) the calculated conformation of the active site in solution is not in accordance with the receptor bond conformation, and the three peptide analogues may possess different abilities to assume conformational transitions to fit the receptor.

Structure−activity investigations on a large number of cyclic pentapeptides of the sequence c(RGDXY) showed that a hydrophobic amino acid in position 4 increases the activity.[29c] Therefore, the low activity of **PA3** could be explained by the missing hydrophobic side chain in the region of the carbon atoms C^4 and C^5 of the BTD motif, which corresponds with position 4 in the cyclic RGD-containing pentapeptides. But the active peptide analogues **PA1** and **PA2** with the ANC moiety do not possess a hydrophobic side chain in this region, too.

Thus, the different activities of these three peptide analogues may result from different possibilities to fit the active site of the receptor. The different fitting abilities are based on the

(60) Hann, M. M.; Carter, B.; Kitchin, J.; Ward, P.; Pipe, A.; Broomhead, J.; Hornby, E.; Forster, M.; Perry, C. In *Molecular Recognition: Chemical and Biochemical Problems II*; Roberts, S. M., Ed.; Royal Society of Chemistry: Cambridge 1992; pp 145−160.

(61) Müller, G.; Gurrath, M.; Kessler, H. *J. Comput.-Aided Mol. Design* **1994**, *8*, 709−730.

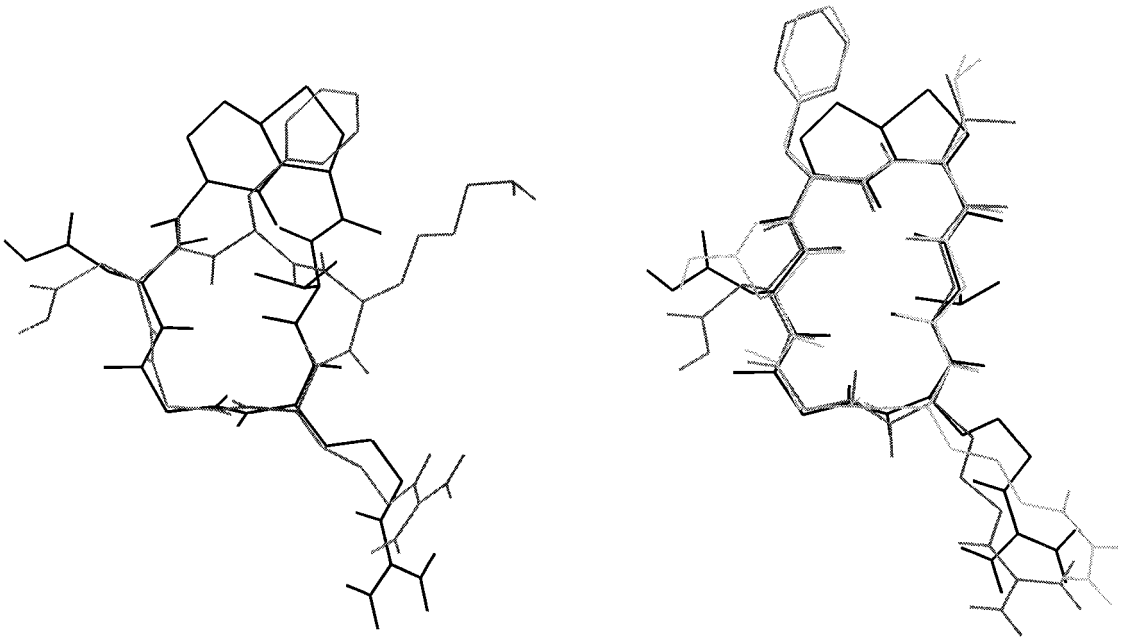

Figure 7. Superimposing of c(RGDFk) (gray) and **PA5** (black; left side) and c(RGDfVG) and c(RGDfLG) (both gray) and **PA5** (black; right side).

increasing flexibility of the peptide analogues. Compound **PA3** with the BTD motif fixes two backbone dihedral angles which leads, according to the design, to a more rigid peptide derivative than the homodetic cyclic pentapeptides. This can be seen, for example, in well-separated temperature coefficients (Table 1). The ANC motif in peptide analogues **PA1** and **PA2** fixes only one backbone dihedral angle and, therefore, reduces the flexibility of the peptides to a smaller extent. **PA2** shows the highest flexibility, which is indicated, for example, via less separated temperature coefficients (Table 1) and a lower convergence of the generated DG structures.

The only difference of peptide analogues **PA1** and **PA2** is focused on the orientation of the carbonyl group of the ANC moiety (see also above). Besides the high flexibility of **PA2**, this different orientation of the carbonyl group could be a reason for the extreme high activity of compound **PA2**, because the carbonyl oxygen could possibly interact as a hydrogen-bond acceptor with the receptor.

The peptide analogue **PA4** shows no activity in the limits of the test system. This is somewhat surprising as the structure of this compound reveals the desired βII′/γ-turn arrangement with the turn mimetic in the $i + 1$ and $i + 2$ positions of the βII′-turn and Gly^2 in the $i + 1$ position of the γ-turn. Especially the region of the RGD sequence is very similar to the conformation of the active site in the lead structure c(RGDfV), which by contrast possesses a very high activity (Table 2). This drastic loss of activity can be explained by the missing hydrophobic side chain in the region of the spiro compound in combination with the absence of an amide proton at the peptide bond between Asp^3 and the turn motif. In recent investigations this amide proton was found to be essential for high activity.[29c] In addition, the introduction of the turn mimetic to reduce the flexibility could prevent the matching of the RGD site with the receptor.

Altogether, these results suggest that the receptor-bound conformation of the RGD sequence differs from the structure found in solution for peptide analogues **PA1**, **PA2**, **PA3**, and **PA4** and that the different analogues possess different abilities to match the receptor due to their different flexibilities. Moreover, these findings show again that a reduction in flexibility can prevent activity when the pharmacophores are fixed in a mismatched conformation. Nevertheless, the incorporation of the RGD sequence in cyclic pentapeptides or peptide analogues which reduce the torsional freedom of the φ-angle in a large amount[61] still results in compounds with highly increased activity for the $\alpha_V\beta_3$-integrin compared to the linear standard peptide GRGDSPK.[62] Thus, often a balance between conformational restrictions and flexibility is the better approach to develop highly active compounds, but does not lead to a better understanding of the ligand−receptor interactions.

It is not surprising that the RaD-containing **PA6** shows no activity, as earlier investigations[63] revealed that the replacement of Gly with D-Ala leads to a drastic loss of activity. But more interestingly, **PA5** shows an activity in inhibiting the binding of vitronectin to the $\alpha_V\beta_3$-receptor in the same range as homodetic cyclic pentapeptides of the sequence c(RGDFx)[29c] and is hence about 10-fold more active than hexapeptides with analogous conformations[31b] like c(RGDfVG) and c(RGDfLG). One explanation for this result could be that the BTD moiety in peptide analogue **PA5** is able to replace the hydrophobic side chain of the comparably active c(RGDFk) (Figure 7) and can interact with the same hydrophobic pocket of the receptor. By contrast, the side chain of the phenylalanine of c(RGDfVG) and c(RGDfLG) is too far away to adopt the same position as in c(RGDFk) (Figure 7).

Conclusion

The conformational analysis of peptide analogues **PA1**−**PA4** (pentapeptide derivatives) shows that only the incorporation of the spiro moiety in c(RGD"spiro") results in the desired βII′/γ-turn arrangement with the turn motif in the βII′-turn. The other three peptide analogues with the S- and *R*-ANC as well as the BTD moiety reveal conformations in which Gly^2 adopts the $i + 1$ position of the βII′-turn while the turn motif is shifted in the $i + 3$ and $i + 4$ position. These unexpected results may be due to the adaptability of the pentapeptide system, which allows the turn mimetics to be located in other positions. Especially, the γ-turn region is very flexible and is therefore predestinated to match the structural demands of the turn mimetics.

The structures of the pseudo-hexapeptide derivatives **PA5** and **PA6** exhibit a βII′/βII-turn arrangement with the BTD moiety

(62) See refs 27c, 28 and 29.
(63) See refs 31a and 33.

in the desired $i + 1$ and $i + 2$ position of the βII′-turn. These results suggest that the turn motif adopts the position for which it was designed in the hexapeptide system, even if there is a competition with a likewise turn-inducing D-amino acid which is shifted into the unfavorable $i + 2$ position of the β-turn.

Structure−activity investigations show inhomogenous results. Whereas in peptide analogues **PA1**, **PA2**, and **PA3** the conformation of the active RGD site is very similar they reveal very different activities concerning the inhibition of binding of vitronectin to the $\alpha_V\beta_3$-receptor. In addition, peptide analogue **PA4**, which possesses a βII′/γ-turn conformation similar to the highly active lead structure c(RGDfV), shows no activity on this receptor. These findings suggest that the structures determined for the peptide analogues examined in solution may differ from the receptor bound conformation, which is probably adopted upon binding via an induced fit. The different activities could be explained with different possibilities for conformational transitions which allow the distinct peptide analogues to match the receptor in different ways. These fitting abilities are determined by the decreasing flexibility induced by the single turn motives. Moreover, the drastic loss of activity of **PA4** confirms recent findings[29c] which postulate that the proton at the amide bond between Asp^3 and the following residue is essential for high activity.

Although these investigations could not improve our understanding of ligand-receptor interactions at the $\alpha_V\beta_3$-integrin, incorporation of the *R*-ANC moiety into the RGD peptide led to one of the compounds most active in inhibiting the binding of vitronectin to the $\alpha_V\beta_3$-receptor. This peptide analogue could be a prospective candidate for further drug developments targeting the interactions of integrin essential during osteoporosis, angiogenesis, and tumor metastasis.

Experimental Section

Materials and Methods. All chemicals were used as supplied without further purification. Apart from *N*-methylpyrrolidone (NMP), all organic solvents were distilled before use. Fmoc amino acids were purchased from Bachem (Heidelberg, Germany) and Novabiochem (Bad Soden, Germany), the Fmoc-(*S*,*S*)-spiro-Pro-Leu-OH was from Neosystems (Strasbourg, France), cTrt resin was from either Novabiochem or CBL Patras (Patras, Greece), Fmoc-Gly-Tentagel S PHB was from Rapp Polymers (Tübingen, Germany), and TBTU was from Richelieu Biotechnologies (Montreal, Canada). HOBt was synthesized using the route described by König and Geiger.[64]

Solvent systems for TLC were acetonitrile/water 4:1 (AW), *n*-butanol/acetic acid/water 2:1:1 (BAW), and chloroform/methanol/acetic acid 85:10:5 (CMA). FAB mass spectra were obtained by a Varian MAT 311 A or a Vacuum Generator VG 70-250SE mass spectrometer using nitrobenzyl alcohol or glycol matrices.

Analytical reverse phase HPLC was performed using columns with Macherey-Nagel Nucleosil C-18 packing (5 μm, 250 × 4 mm) or a Lichrosorb RP18 (5 μm, 250 × 4 mm) column. For analytical data, given as K', several acetonitrile (ACN)/0.1% aqueous trifluoroacetic acid gradients are used (see supporting information).

Synthesis of the BTD Moiety: Phth-BTD-OH. To 2.30 g (6.1 mmol) of Phth-BTD-OEt[65] in 130 mL of acetic acid, was added 30 mL of concentrated HCl and the solution was allowed to reflux for 90 min. The solvent was evaporated at room temperature, and the product was obtained as a white solid: yield 2.12 g (99%) (95% pure according to HPLC); HPLC $K' = 5.97$ (20-80% ACN; 30 min); ^{1}H-NMR (DMSO-d_6) δ 7.85−7.93 (m, 4H), 5.05 (dd, 1H), 4.95 (dd, 1H), 4.80 (dd, 1H), 3.45 (dd, 1H), 3.10 (dd, 1H), 1.90−2.50 (m, 4H); FAB-MS $[M + H]^+ = 347$.

H-BTD-OH. To a stirred solution of 2.12 g (6.1 mmol) of Phth-BTD-OH in 15 mL of chloroform and 170 mL of 95% ethanol was added 1.35 mL of hydrazine hydrate. The reaction mixture was stirred for 24 h at ambient temperature, filtered, and washed with 95% ethanol. The filtrate was evaporated to dryness under reduced pressure: yield 1.3 g (96%); mp = 265 °C; TLC $R_{f(BAW)} = 0.83$; HPLC $K' = 3.79$ (10-60% ACN; 30 min); ^{1}H-NMR (DMSO-d_6) δ 8.30 (s, 3H), 4.95 (dd, 1H), 4.85 (dd, 1H), 4.00 (m, 1H), 3.45 (dd, 1H), 3.10 (dd, 1H), 1.80−2.40 (m, 4H); FAB-MS $[M + H]^+ = 217$.

Fmoc-BTD-OH. To a stirred solution of 1.27 g (5.9 mmol) of H-BTD-OH in 20 mL of water was added 2.0 g (5.93 mmol) of Fmoc-ONSu dissolved in 20 mL of acetonitrile. The pH was maintained at pH 8.0 using triethylamine. The solution was stirred for 30 min at ambient temperature. The mixture was filtered and concentrated *in vacuo*. The residue was added with rapid stirring to 100 mL of 1.5 N HCl. The crystallizing product was collected by filtration, washed with water, and dried *in vacuo*: yield 1.50 g (57%); mp = 210 °C; TLC $R_{f(AW)} = 0.63$; HPLC $K' = 4.83$ (30−90% ACN; 30 min); ^{1}H-NMR (DMSO-d_6) δ 7.87 (d, 2H), 7.67 (m, 3H), 7.28−7.43 (m, 4H), 4.85−4.96 (m, 2H), 4.22−4.29 (m, 3H), 4.09 (dd, 1H), 3.39 (dd, 1H), 3.05 (dd, 1H), 1.79−1.97 (m, 4H); FAB-MS $[M + H]^+ = 439$.

Synthesis of PA1, PA2, and PA4: Peptide Synthesis. Fmoc-Gly-Tentagel S PHB was used in the 9050 peptide synthesizer (Milligen, Eschborn, Germany). Protected amino acids (Fmoc-Arg(Mtr)-OH, Fmoc-Asp(OtBu)-OH) and building blocks (**PA1**, Fmoc-(*S*)-Gly[ANC-2]Leu-OH; **PA2**, Fmoc-(*R*)-Gly[ANC-2]Leu-OH; **PA4**, Fmoc-(*S*,*S*)-spiro-Pro-Leu-OH) were used in 4-fold excess. The synthetic protocol was essentially as described by the manufacturer.

Cleavage. After completion of the coupling cycles and deprotection of the Fmoc group of the Asp residue, the peptide was cleaved from the resin as described previously.[66] The linear protected peptides were cyclized without purification.

Cyclization. The linear peptide was dissolved in CH_2Cl_2/DMF (1 mg/mL) and cooled to −10 °C. One equivalent of *N*-methylmorpholine and DMAP and 2 equiv of EDCI·HCl were added successively. The solution was stirred for 2 h at −10 °C and overnight at room temperature. After evaporation, 2−3 mL of DMF was added and the concentrated solution was poured into water. The precipitate was sucked off.

Side Chain Deprotection. Deprotection of the Mtr group at arginine and the *tert*-butyl ester of asparagine was performed with TFA/10% thioanisole.

Purification. Final purification was achieved by preparative RP-HPLC using a Prepbar Lichrosorb RP18 (10 μm, 250 × 50 mm) column. The gradient was 5 min 5% B in 50 min to 75% B [(A) 0.1% TFA, (B) 0.1% TFA in water/acetonitrile 1:9]. All peptides were >95% pure.

Synthesis of PA3, PA5, PA6: Loading of the cTrt Resin. A 0.7 g portion of cTrt resin suspended in 10 mL of dry DCM was treated with 0.74 g (2.5 mmol) of Fmoc-Gly-OH and 400 μL of DIEA for 1 h. After adding another 400 μL of DIEA and 3 mL of methanol the mixture was shaken further 15 min. The solution was removed and the resin was washed several times with DMF (2×), DCM (5×), 2-propanol (2×), methanol (5×), and ether (2×).

Peptide Synthesis. Starting with 0.8−0.9 g of Fmoc-Gly-cTrt resin (substitution about 0.55−1.10 mmol amino acid/g resin), the synthesis was carried out using standard Fmoc coupling protocols. Deprotection of the N-terminal Fmoc group was accomplished using 20% piperidine in DMF. Coupling of the amino acids or amino acid derivative was carried out using 2.5 equiv of the appropriate amino acid or 1.5 equiv of amino acid derivative, 2 equiv of TBTU, 2.5 equiv of HOBt, and 3−5 equiv of DIEA in 20 mL of NMP. Coupling times between 30 and 60 min provide complete couplings. Coupling reactions were monitored by the ninhydrin test.[67]

Acetic Acid Cleavage. The resin bound peptide analogue was treated with 20 mL of a mixture of acetic acid, TFE, and DCM (1:1:3) for 1 h at ambient temperature. The resin was washed twice with 20 mL of the mixture mentioned above. The combined solution was evaporated *in vacuo* and triturated with ether, filtered, and washed three times with ether.

(64) König, W.; Geiger, G. *Chem. Ber.* **1970**, *103*, 788−798.

(65) The synthesis of Phth-BTD-OEt follows the scheme of Bach et al. (see ref 37e) and was slightly modified using EDCI·HCl as coupling reagent in the synthesis of the ethyltrimethylsilyl protected glutamic acid.

(66) (a) Anwer, M. K.; Spatola, A. F.; Bossinger, C. D.; Flanigan, E.; Liu, R. C.; Olsen, D. B.; Stevenson, D. *J. Org. Chem.* **1983**, *48*, 3505−3507. (b) Hölzemann, G.; Löw, A.; Harting, J.; Greiner, H. E. *Int. J. Pept. Protein Res.* **1994**, *44*, 105−111.

(67) Troll, W.; Cannan, R. K. *J. Biol. Chem.* **1953**, *200*, 803−811.

Cyclization. The peptide analogue was dissolved in DMF (concentration 5×10^{-3} mol/L), 5 equiv of $NaHCO_3$ and 3 equiv of DPPA were added, and the solution was stirred at ambient temperature for 24 h. After filtration of the solid $NaHCO_3$, DMF was evaporated *in vacuo* and the residue was triturated with water, filtered, and washed with water and ether.

Side Chain Deprotection. The cyclic peptide analogue was treated with 20 mL of a solution of 85.5% TFA, 5% phenol, 2% water, 5% thioanisole and 2.5% ethanedithiol for 24 h at ambient temperature. The mixture was filtered if necessary, evaporated *in vacuo*, triturated with ether, filtered, and washed several times with ether.

Purification. The crude, cyclic peptide analogues were purified by RP-HPLC using a 250 mm × 21 mm column containing a Nucleosil C-18 packing (7 μm, 100 Å pore size). Eluation from the column is done with several linear acetonitrile/0.1% aqueous TFA gradients. All peptides were >95% pure.

NMR Spectroscopy. All NMR spectra were recorded on a Bruker AMX 500 spectrometer and processed on an Aspect X32 station with the UXNMR software (Bruker). Measurements were performed using 20 mM solutions of the peptides in DMSO-d_6 at 300 K sealed under *vacuo* after three pump-and-freeze cycles. The TOCSY spectrum for **PA1** was recorded with 2048 data points in the direct dimension and 512 experiments using an 80 ms MLEV-17 spinlock. It was processed by applying a π/2-shifted squared sine bell window function in both dimensions and zero-filling in F_1 to a final size of 2048 × 11024 data points. For the other peptides, *z*-filtered TOCSY spectra with an 80 ms DIPSI spinlock and 11 different variable delays for each experiment were recorded with 8192 data points in the direct dimension and 512 experiments using TPPI. After application of a squared sine bell function, shifted by π/2, they were zero-filled to a final size of 8192 × 1024 points. For P.E.COSY experiments (8192 × 512 data points) a 37° reading pulse was applied. After the subtraction of the one-dimensional reference spectrum and multiplication with a π/2-shifted squared sine bell, the spectra were zero-filled in F_1 to a size of 8192 × 1024 data points. The heteronuclear HMQC spectra (1024 × 512 points) have been recorded using a BIRD pulse to suppress protons bound to ^{12}C with a recovery delay of 198 ms. HMQC-TOCSY experiments were measured under the same conditions but with an additional MLEV-17 spinlock with a mixing time of 80 ms. HMBC spectra (8192 × 384 data points) with a delay of 70 ms for the evolution of the heteronuclear long-range coupling have been folded in the F_1-dimension to increase the resolution. The first increment was adjusted to obtain a phase correction of 180° (zero-order) and −360° (first-order) in the indirect dimension. For the heteronuclear spectra, a squared sine bell shifted by π/2 was applied in F_2 before Fourier transformation to a final size of 2048 × 512. For compounds **PA5** and **PA6** HETLOC spectra were recorded with 8192 data points in F_2 and 512 experiments using a mixing time of 35 ms with the MLEV-17 spinlock. Prior to the Fourier transformation a π/2-shifted squared sine bell window function was applied. NOESY spectra for **PA1** and **PA3** were recorded with mixing times of 150 ms, and compensated ROESY spectra were recorded for the other peptides with a mixing time of 200 ms using a pulsed spinlock with 3 kHz (4096 × 512 data points). After processing (π/2-shifted squared sine bell, zerofilling in F_1 to 1024 points) the volume integrals of the crosspeaks were measured using the integration subroutine of the UXNMR-program (Bruker). Distances have been calculated using the isolated two-spin approximation with reference to the distance between two geminal protons set to 178 pm. For the volume integral values of the compensated ROESY spectra an offset correction was performed.

Biological Assay: Protein Purification. Human plasma vitronectin[68] and fibrinogen[69] were purified as described previously. $\alpha_V\beta_3$-integrin was purified from human placenta[70] with modifications.[71] Briefly, human placenta was extracted with octyl β-D-glucopyranoside (OG) at 4 °C. The extract was cleared by centrifugation and circulated over an LM609 antibody column[72] and specifically bound material was eluted at pH 3.1. The eluant was neutralized, dialyzed against NP-40 (0.1% in PBS), concentrated to >1 mg/mL, and stored at −70 °C.

$\alpha_{IIb}\beta_3$-integrin was prepared from human platelets[73] with modifications.[71] Briefly, platelets were extracted with OG (50 mM). The extract was circulated over a linear GRGDSPK-conjugated CL-4B Sepharose column, and specifically bound material was eluted with linear GRGDSPK. The eluant was dialyzed against NP-40 (0.1% in PBS), concentrated to >1 mg/mL, and stored at −70 °C.

Both preparations were ∼95% pure as judged by anti-integrin ELISA using α- and β-chain specific monoclonal antibodies and by SDS−PAGE.

Isolated Integrin Binding Assays. Inhibitory effects of cyclic peptides were quantified by measuring their effect on the interactions between immobilized integrin and biotinylated soluble ligands. Purified vitronectin or fibrinogen (1 mg/mL; pH 8.2) was biotinylated with *N*-hydroxysuccinimidobiotin (100 μg/mL; 1 h, 20 °C), before dialysis into PBS. Ninety-six-well mictrotiter plates were coated with 1 μg/mL of purified integrin (1 h; 4 °C), blocked with BSA (1% in PBS), and incubated [3 h at 30 μg/mL in binding buffer (0.1% BSA, 1 mM $CaCl_2$, 1 mM $MgCl_2$, 10 μM $MnCl_2$, 100 mM NaCl, 50 mM tris(hydroxymethyl)aminomethane; pH 7.4)] in the presence or absence of serially diluted peptides. After washing (3 × 5 min with binding buffer), bound biotinylated ligand was detected with alkaline-phosphatase conjugated to goat-anti-biotin antibodies (1 μg/mL; 1 h, 37 °C), using nitro blue tetrazolium−bromochloroindolyl phosphate as chromogen. Vitronectin binding in the absence of competitor was defined as 100% signal, binding to blocked wells in the absence of integrin was defined as 0%. The signal-to-noise ratio was >10. Concentrations of peptides required for 50% inhibition of signal (IC_{50} values) were estimated graphically. The linear heptapeptide GRGDSPK was included as external reference, and IC_{50} values within a given experiment were normalized to the reference IC_{50} to give a value, '*Q*', which allowed IC_{50} between experiments to be compared.

Acknowledgment. Financial support by the Deutsche Forschungsgemeinschaft and the Fonds der Chemischen Industrie is gratefully acknowledged. The authors thank M. Nowee, H. Kraft, and D. Hahn for excellent technical support; H. Müller for contributing the FAB-mass spectra; and M. Kranawetter, B. Cordes, and M. Wurl for HPLC separations.

Supporting Information Available: Additional tables with ^1H- and ^{13}C-chemical shift data for all peptide analogues, selected homonuclear and heteronuclear ^3J coupling constants, comparisons between experimentally determined and simulated NOE-derived distances of all peptide analogues, and analytical data such as FAB masses, HPLC retention times, and yields of the peptide analogues (17 pages). See any current masthead page for ordering and Internet acess instructions.

JA9608757

(68) Yatohgo, T.; Izumi, M.; Kashiwagi, H.; Hayashi, M. *Cell Struct. Funct.* **1988**, *13*, 281−292.
(69) Kazal, L. A.; Ansel, S.; Miller, O. P.; Tocantins, L. M. *Proc. Soc. Exp. Biol. Med.* **1963**, *113*, 989−994.
(70) Smith, J. W.; Cheresh, D. A. *J. Biol. Chem.* **1988**, *263*, 18726−18731.
(71) Mitjans, F. C.; Sander, D.; Adán, J.; Sutter, A.; Martinez, J. M.; Jäggle, C.; Moyano, J. M.; Kreysch, H.; Piulats, J.; Goodman, S. L. *J. Cell Sci.* **1995**, *108*, 2825−2838.
(72) Cheresh, D. A.; Spiro, R. C. *J. Biol. Chem.* **1987**, *262*, 17703−17711.
(73) Pytela, R.; Pierschbacher, M. D.; Ginsberg, M. H.; Plow, E. F.; Ruoslahti, E. *Science* **1986**, *231*, 1559−1562.